Científica

vol. 30, no. 1, January-June 2026, pp. 01-28
ISSN 2594-2921, Instituto Politécnico Nacional, MÉXICO
e300106 | DOI: 10.46842/ipn.cien.v30n1a06

ARTICLE

Validation of the prototype of L-CADEL.v5 elbow assisting device

Validación del prototipo del dispositivo L-CADEL.v5 de asistencia para el codo

Sergei **Kotov** [1]
Marco **Ceccarelli** [2]

University of Rome Tor Vergata,
Department of Industrial Engineering,
Rome, ITALY

[1] ORCID: 0009-0003-5018-4442 / sergei.kotov@students.uniroma2.eu
[2] ORCID: 0000-0001-9388-4391 / marco.ceccarelli@uniroma2.eu

https://científica.site

Recibido 25/04/2026, aceptado 28/05/2026.

Abstract

This paper presents the validation of the L-CADEL v5 elbow assisting device, developed from previous versions to improve its functional effectiveness and the accuracy of its kinematic measurements. The work is based on laboratory testing results involving 100 healthy volunteers performing standardized elbow flexion and extension movements. Kinematic analysis of movements was conducted using three independent systems: the device's integrated IMU sensor data, motion analysis using Kinovea software, and an artificial intel-ligence-based motion analysis system. A quantitative comparison of results from the various systems is presented to assess measurement consistency and identify potential systematic discrepancies.

Index terms: dry abrasion, silica sand, austenite, stainless steel, high temperature.

Resumen

Este artículo presenta la validación del dispositivo L-CADEL v5 de asistencia para el codo que se ha desarrollado a partir de versiones anteriores para mejorar su eficacia funcional y precisión de sus mediciones cinemáticas. El trabajo se basa en los resultados de pruebas de laboratorio realizadas con 100 voluntarios que ejecutaron movimientos estandarizados de flexión y extensión del codo. El análisis cinemático de los movimientos se llevó a cabo mediante tres sistemas independientes: los datos del IMU sensor integrado del dispositivo, el análisis de movimiento con el software Kinovea y un sistema de análisis de movimiento basado en inteligencia artificial. Se presenta una comparación cuantitativa de los resultados obtenidos por los distintos sistemas para evaluar la consistencia de las mediciones e identificar posibles discrepancias sistemáticas.

Palabras clave: abrasión seca, arena de sílice, austenita, acero inoxidable, alta temperatura.

I. INTRODUCTION

The elbow joint plays a vital role in human functional activity, participating in a wide range of everyday, professional, and athletic tasks. Limited mobility or impaired elbow biomechanics, resulting from traumatic injuries, surgical interventions, or neurological diseases, can significantly reduce a patient's functional capabilities and quality of life. Therefore, elbow rehabilitation [1] is an important area of modern orthopedics, traumatology, and neurorehabilitation. Restoring range of motion after fractures, dislocations, surgeries, or neurological disorders requires systematic monitoring and objective assessment of functional recovery dynamics. In this context, the development and implementation of assistive rehabilitation devices is of significant scientific and practical interest.

Traditionally, elbow rehabilitation relied on passive mechanotherapy [2] and on a specialist's subjective visual assessment of the patient's condition. Subsequently, articulated orthoses with adjustable motion parameters were developed, as well as mechanical continuous passive motion (CPM) systems [3] that allow for amplitude and load control. However, most of these devices did not allow quantitative real-time recording of kinematic parameters or the acquisition of digital data for subsequent analysis of the recovery process.

The development of robotic technologies [4] and motion capture systems has enabled the emergence of more advanced solutions for upper-limb rehabilitation [5]. Robotic systems [6] such as Armeo and Biodex, as well as other stationary rehabilitation platforms, provide highly accurate kinematic parameter recording and the ability to deliver controlled therapy. However, the cost of such systems, which can reach tens of thousands of euros, the need for specialized equipment, personnel training, and regular maintenance significantly limit their use. Furthermore, these systems are bulky and primarily intended for use in large medical facilities, limiting their availability for long-term home rehabilitation.

Similarly, professional optoelectronic motion capture systems, including Vicon and Qualisys, provide benchmark accuracy in spatial motion analysis. However, their cost can exceed €100,000 and require multi-camera systems, physical markers, and strict environmental control. Despite their high measurement accuracy, such systems have limited practical applicability for routine clinical practice and home rehabilitation.

Therefore, there is a need to develop accessible, portable, and cost-effective solutions [7], [8], [9] capable of objectively recording kinematic parameters in elbow rehabilitation. This study presents the L-CADEL v5 prototype [10], [11], [12] — an elbow rehabilitation assistive device designed to combine mechanical support with digital motion monitoring. The device consists of three main components and uses an inertial measurement unit (IMU) to measure the forearm's spatial orientation and calculate angular parameters in real time. The system also receives data from Dynamixel servo motors to monitor the device's performance.

One of the main advantages of the L-CADEL v5 is its compact size, portability, and relatively low cost of approximately €180. These features make the system potentially accessible to a wide range of users, including outpatients and participants in home rehabilitation programs. The device's design ensures secure fixation on the user's limb and minimizes unwanted platform movement during exercise.

To objectively evaluate the accuracy and reliability of the L-CADEL v5 prototype, this study conducted a comparative analysis using three different motion assessment methods. The first approach utilized data from the device's inertial sensors to calculate the tilt angle as the primary parameter of elbow flexion and extension. The main advantages of this approach are its autonomy, independence from external recording systems, and real-time operation.

The second approach involved video analysis with Kinovea, a widely used software tool in sports biomechanics. The L-CADEL v5 system has been widely used in clinical trials and clinical studies due to its accessibility and ease of use. This system enables manual or semiautomated determination of joint points and calculation of angles in a two-dimensional plane, providing reproducible visual assessment of kinematic characteristics.

The third method used a computer vision system with elements of artificial intelligence to detect anatomical landmarks and calculate joint angles in two and three-dimensional space without the use of physical markers. The advantage of this approach is the high level of automation of data processing, especially when working with large volumes of data. However, the accuracy of such systems may be dependent on shooting conditions, lighting parameters, and the specifics of the recognition algorithms used.

Therefore, the aim of this study is to evaluate the effectiveness and applicability of L-CADEL v5 as an assistive device for elbow rehabilitation through a comparative analysis of inertial sensor data with video analysis and computer vision methods based on artificial intelligence. Comparing the dynamics of parameter changes, value ranges, and average movement profiles enables us to evaluate the accuracy of the developed prototype and determine its potential for use in clinical practice and home rehabilitation settings.

II. MATERIALS AND METHODS

This section describes the engineering concept, design implementation, and experimental validation of the L-CADEL v5 assistive device for elbow rehabilitation. It describes the system development requirements that determined its functional, ergonomic, and technical characteristics, and presents the prototype architecture, describing its mechanical structure, sensor integration, actuator modules, and control system. A standardized video recording protocol is described, ensuring reproducible measurements and accurate calculation of angular motion parameters. This comprehensive methodological approach enables an objective assessment of the device's accuracy, stability, and practical applicability during cyclic elbow flexion and extension exercises.

A. Design requirements

The development of assistive devices for the elbow requires formalized requirements based on clinical [13], engineering [14], and operational [15] criteria. Unlike large robotic systems, the device must be designed for portability, accessibility, and integration with digital motion analysis tools [16]. For the L-CADEL v5, the requirements were developed based on its purpose as a compact device designed to actively assist elbow flexion and extension while simultaneously monitoring kinematic parameters [17-20]. Figure 1 presents the key requirements that determined the prototype's architecture and functionality:

- Clinical Functionality and Biomechanical Correctness. Ensuring controlled elbow flexion and extension with the ability to set limiting angles of motion will prevent joint overload during exercise. The system must provide adjustable mechanical motion support via servomotors (Dynamixel), partially or fully compensating for the patient's muscular impairment. Pitch angle recording is essential as the primary parameter for elbow joint kinematics, enabling data to be saved for subsequent analysis of therapy progress.
- Mechatronic. Sensors placed on the user's body will provide stable registration of the user's movement, acceleration components, and angles, with a sampling frequency of approximately 100 Hz. The microcontroller, as the heart of the system, must provide real-time data processing, including angle cal-culation, signal filtering, and servo motor control to ensure the exercise is performed correctly. Control algorithms should ensure

synchronicity between angle measurement and servomotor operation to prevent delays and incorrect system responses. The system should support recording data to a microSD card and transmitting it via a Web Interface for post-processing.

- Ergonomic and Mechanical Design. The platform geometry should match the anatomy of the limbs and ensure comfort during long-term use. The design must be lightweight, modular, and adaptable to the user's various anthropometric parameters. The device's overall weight should be minimized to reduce user strain, especially for those with weakened muscles. Comfort during cyclic exercises and the ability to be worn over clothing are important performance criteria. It is also desirable for the device's design to be modular, allowing the replacement of individual components without a complete redesign of the system.
- Safety and Operational Reliability. Software and hardware limitations on angles of motion should be provided to prevent hyperextension or excessive flexion. Electrical safety is an important parameter to ensure safe, low-voltage operation without risk to the user (9V battery). Components must maintain stable operation over extended sessions. Using Fail-Safe Mechanisms will improve the device's safety.
- Accessibility and Cost Efficiency. Using affordable components will reduce the device's cost, making it accessible to users while maintaining functionality comparable to that of more expensive systems. The device should be self-contained, compact, and suitable for home use without complex calibration. Integration with a web interface for remote monitoring, real-time data visualization, and storage of experimental results will support telerehabilitation and expand the system's clinical capabilities.
-

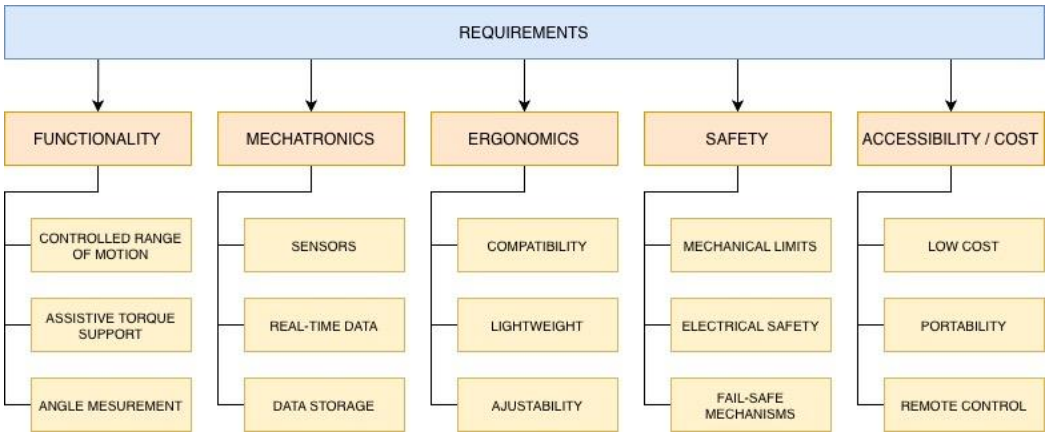

Fig. 1. Main requirements for L-CADEL v.5 assisting device.

The requirements formulated reflect a balance between clinical appropriateness, engineering reliability, user comfort and cost-effectiveness. This design requirements structure will enable the creation of a prototype as a compact, functional, and affordable assistive device for elbow rehabilitation with an integrated digital motion analysis system.

B. L-CADEL v5 Design

The L-CADEL version 5 device was developed in accordance with the previously described requirements, aiming to provide safe, reproducible, and objective support for elbow joint motion during rehabilitation. The prototype is a wearable electromechanical device designed to assist elbow flexion and extension movements within a range of 0° to 140°, which corresponds to the functional range of motion used in most rehabilitation protocols.

The system consists of three functional platforms: the Arm Platform, which is fixed to the forearm; the Wrist Platform, which is secured to the wrist; and the Control Platform, which contains the controls and electronics. This modular architecture provides design flexibility, simplifies adaptation to the user's anatomical features, and improves comfort during long-term use. The system's drive is implemented using two Dynamixel 12A servomotors, selected for their high positioning accuracy, stable torque, and smooth operation, which are critical for assisting devices that interact with the user. Force is transmitted from the servomotors to the wrist platform via a cable mechanism, ensuring controlled wrist movement and, consequently, elbow joint rotation in the sagittal plane. The control system is based on an ESP32 microcontroller that collects, processes, and transmits data in real time from sensors on the Arm Platform and Wrist Platform. The user interface consists of an integrated display and a web interface, enabling tracking of exercise progress and key movement parameters. The acquired sensor data is used both to analyze the kinematics of the user's movements and to evaluate the correct operation of the servomotors and the system.

Figure 2(a) shows the conceptual design of the prototype. The Arm Platform is a flexible ring structure with radius R_a, fixed to the user's and. Servomotors M1 and M2 are located on either side of the platform. The Wrist Platform is also flexible ring with radius R_β and is connected to the servomotors via cables L1 and L2, secured at points A and B. This configuration converts the servomotors' rotational motion into controlled flexion and extension of the elbow joint. An inertial measurement unit (IMU) on the Wrist Platform records accelerations, orientation, and angular rates. The diagram also shows the coordinate systems used and orientation angles (pitch, Roll, and yaw). Figure 2(b) shows the prototype mounted on the user's arm during one of the laboratory tests conducted at ESIME, University IPN (Mexico). The device's design allows comfortable use with everyday clothing, increasing ease of use and expanding its potential application scenarios, including clinical and semi-home rehabilitation settings.

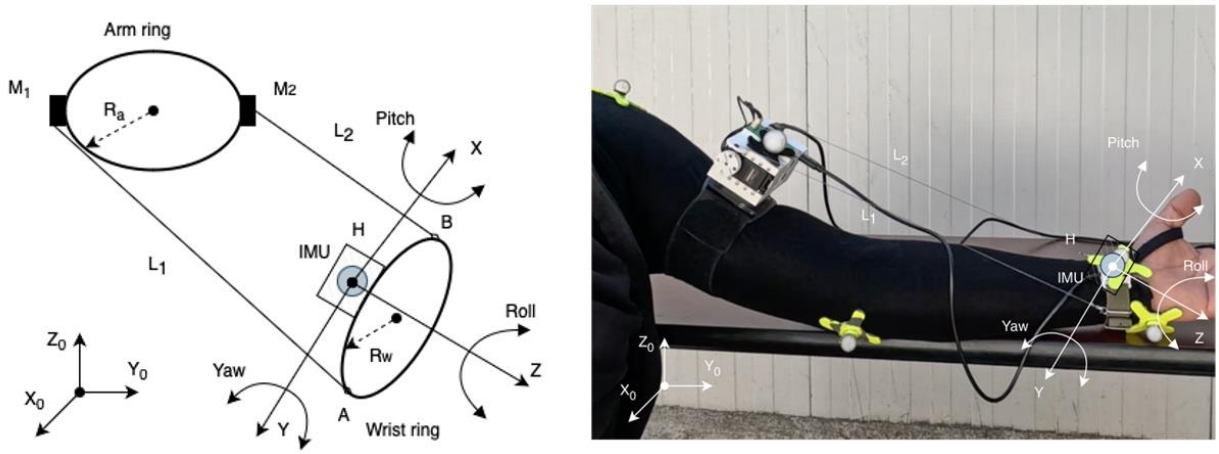

Fig. 2. Design of L-CADEL v.5: (a) Conceptual design; (b) Prototype installed on the arm.

Figure 3 shows the conceptual design of the L-CADEL v5 device as an assistive system for elbow joint rehabilitation. The device architecture includes three main mechanical and electronic subsystems—the Wrist Platform, Arm Platform, and Control Unit—as well as an external visualization and interaction layer via a Web Interface and Display Unit.

The Wrist Platform is mounted on the user's wrist. This platform houses an IMU sensor, which records the spatial orientation of the forearm segment. The Arm Platform is positioned on the upper biceps and performs mechanical and

actuation functions. Two Dynamixel servomotors are installed on this platform. The Control Unit is the central element of the system. It includes a microcontroller that processes data from the IMU sensor, controls the Dynamixel, and implements algorithms to calculate angular parameters. A TFT touchscreen is used for local display of information, allowing the user to view current angle values, the device's operating mode, and training parameters. The system is powered by a standalone 9V battery, ensuring mobility and independence from stationary power sources. A microSD card is provided for data recording and subsequent analysis. Data is transferred from the Control Platform to the external interaction layer, the Web Interface. The Web Interface enables remote monitoring, movement dynamics analysis, storage of training history, and potential integration with telerehabilitation platforms.

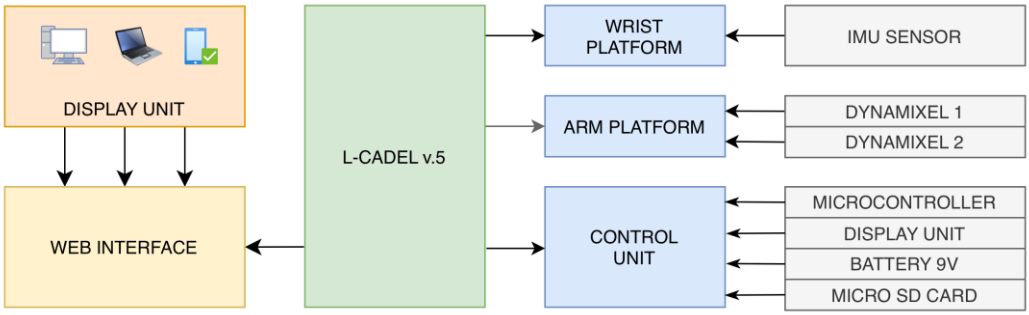

Fig. 3. Conceptual design for L-CADEL v5 with connection to the Web Interface.

Thus, the design reflects the modular architecture of the L-CADEL v5, in which the sensor layer (Wrist Platform) records movement, the actuator layer (Arm Platform) implements the assistive mechanics, and the control layer (Control Unit) processes data, controls the actuators, and communicates with the user. This structure ensures autonomy, mobility, and the ability to monitor the rehabilitation process both locally and remotely, making the device functionally flexible and suitable for both clinical and home use.

B. Protocol for video recording

To generate a reliable, reproducible experimental dataset, a standardized protocol for video recording elbow flexion/extension movements was developed. Approximately 100 volunteers participated in the study, ensuring statistical stability of the sample and accounting for interindividual anatomical and kinematic differences. For each participant, four video sequences were recorded, including movements of the right and left arms in frontal and posterior views. This approach ensures a complete spatial representation of movement, improves the accuracy of visual marker tracking, and enables analysis of elbow joint kinematics in the sagittal plane. Additionally, multi-angle recording improves the quality of the data used for subsequent device validation using Kinovea software and an AI-based system.

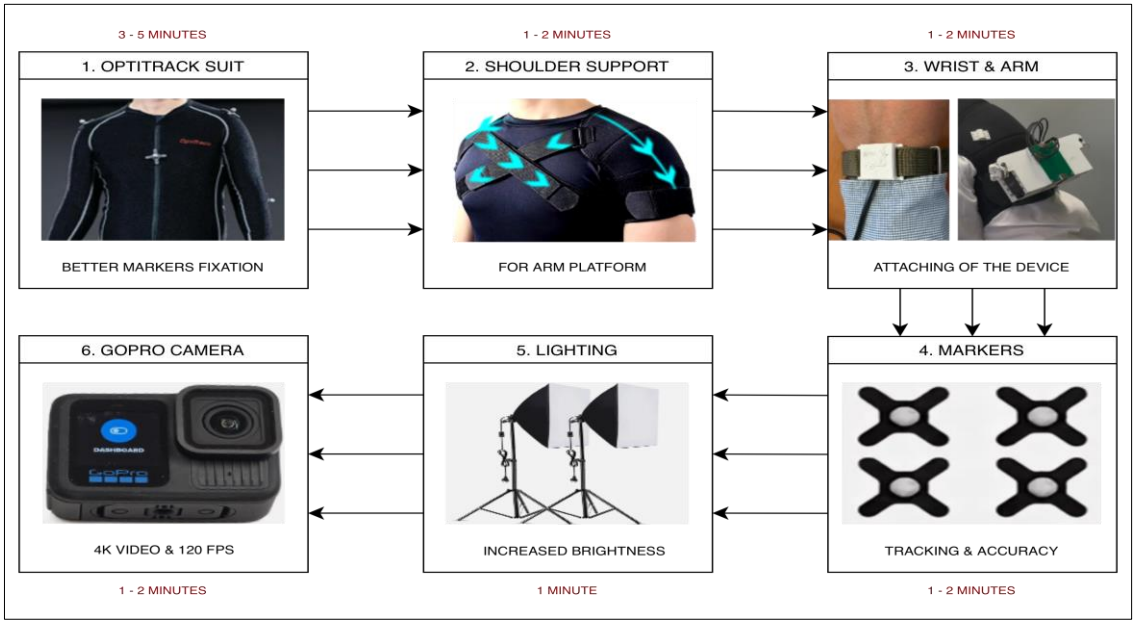

Fig. 4. Steps & Timing for video recording.

Volunteer and equipment preparation followed the step-by-step protocol presented in Figure 4. First, the participant donned special, form-fitting OptiTrack suit, ensuring a snug fit (Step 1, 3–5 minutes). This approach increased marker stability, improved visual readability, and reduced visual noise during subsequent video data analysis. Using OptiTrack suits minimizes the possibility of fabric shifting during exercise. Next, the shoulder support element is installed (Step 2, 1–2 minutes), designed to secure the Arm Platform. This design ensures the Arm Platform remains stable relative to the shoulder segment and improves user comfort during exercise. The shoulder support can be adjusted to suit a variety of user anatomy. Next, the Arm Platform and Wrist Platform are secured to the user's arm (Step 3, 1–2 minutes). The Wrist Platform is attached to the user's wrist using a nylon strap. The Arm Platform is attached to the upper biceps using a plastic base and a metal buckle. After mechanical fixation, all electrical connections and power cables are connected, preparing the device for the exercise.

For subsequent video analysis, visual markers are placed on anatomical landmarks of the upper limb (step 4, 1–2 minutes). Their placement is optimized to improve joint angle tracking accuracy and minimize tracking errors during video processing. The anatomical angle (shoulder-elbow-wrist) and the angle between two platforms (Arm Platform-elbow-Wrist Platform) are analyzed. The lighting equipment is adjusted to ensure uniform illumination of the work area (step 5, 1 minute). Increased brightness and directional lighting reduce shadows, enhance marker contrast, and improve the quality of video data for analysis in Kinovea and AI systems. In the final step, the video camera is installed (step 6, 1–2 minutes). The experiments utilized a GoPro camera capable of recording 4K video at 120 fps and featuring HyperSmooth 6.0 image stabilization. This configuration provides the high temporal and spatial resolution necessary for accurate analysis of movement kinematics.

Thus, the complete video recording process for one volunteer takes an average of 20 to 30 minutes, depending on the participant's anatomical characteristics and the time required for proper equipment setup. This duration includes the entire preparation phase, including donning specialized clothing, securing the shoulder support, installing the L-CADEL v.5 platforms, connecting the electrical connections, placing visual markers, and setting up the lighting and

video camera. This step-by-step setup ensures system stability, accurate measurements, and high-quality recorded data. For each volunteer, four video sequences are recorded, corresponding to movements of the right and left arms in the frontal and posterior projections. Each video sequence includes three consecutive cycles of elbow flexion and extension, performed at a natural pace for approximately 30 seconds per cycle. As a result, each video sequence is approximately 1.5 minutes long, with a total data volume per volunteer of approximately 6 minutes in 4K format at 120 frames per second. This level of detail allows for a fairly accurate analysis of the angular characteristics of movement during exercise.

III. Results

The L-CADEL v5 prototype was experimentally tested in laboratory conditions at IPN University (Mexico City). The tests were conducted as an extended pilot campaign involving over 100 volunteers and aimed to comprehensively evaluate the mechanical design, the control system's reliability, and the device's effectiveness in assisted elbow movements. All participants had intact functional elbow mobility and reported no previous injuries or musculoskeletal conditions.

Table 1 presents the demographic characteristics of the 105 volunteers. The study included 76 men (72%) and 29 women (28%). The average age of the participants was 29 ± 12 years, with a range from 20 to 76 years, indicating a broad age distribution. The largest proportion of subjects was in the 20–30 age group (70%), while the 31–50 and over-51 age groups each accounted for 15%. The average height of the participants was 169 ± 9 cm (142–192 cm), and the average body weight was 74 ± 11 kg (50–120 kg). These data demonstrate heterogeneity in the sample with respect to age and anthropometric parameters, thereby increasing the generalizability of the results when evaluating the performance of the L-CADEL v5 device.

Table 1
Demographic and Anthropometric Characteristics of the Volunteers

	Paramiter	Value
1	Total volunteers	105
2	Male / Female	76 (72%) / 29 (28%)
3	Age (mean +/- sd (min-max))	29 +/- 12 years (20-76)
4	Age (20 - 30 / 31 - 50 / over 51)	70% / 15% / 15%
5	Height (mean +/- sd (min-max))	169 +/- 9 cm (142-192)
6	Weight (mean +/- sd (min-max))	74 +/- 11 kg (50-120)

During testing, volunteers generally rated the prototype's ergonomics and ease of use positively, noting its intuitive controls and the natural feel of the supported movements. Participants also reported a good level of comfort during the cyclic exercises, with no pain or subjective discomfort in the elbow joint. This demonstrates correct kinematic synchronization between the user's hand movement and the device's actuators. The five-frame sequence shown in Figure 19 illustrates a complete cycle of elbow flexion-extension exercise performed by a volunteer using the L-CADEL v5 prototype and clearly demonstrates the movement's stability and repeatability.

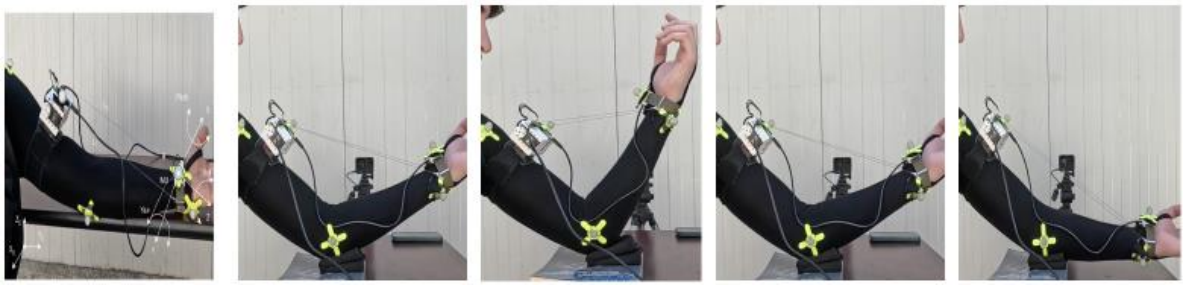

Fig. 5. Snapshots of flexion-extension exercise by a volunteer for elbow testing device L-CADEL v5.

The experiment was conducted according to the protocol described in [32]. The subject's initial position was seated at a table, with the forearm resting on a horizontal surface, as shown in Figure 5. Each volunteer performed three consecutive cycles of elbow flexion and extension at a natural speed of 30 seconds per cycle. Four videos were recorded for each volunteer: right and left arm, front and back views. The MPU 6050 wrist-mounted IMU is used to assess forearm position and record forearm movement in real time during the exercise.

The control algorithm operates with two fixed angular thresholds: 0°, corresponding to maximum elbow extension, and 90°, corresponding to maximum flexion. Upon reaching the upper threshold (90°), the system interprets this state as the completion of the flexion phase and automatically reverses the servomotor rotation direction, initiating the extension phase. Similarly, decreasing the angle to the lower threshold (0°) reverses the direction of movement, ensuring the transition to the next cycle. This enables the implementation of stable periodic motion dynamics between the two limit positions. This control algorithm is characterized by high reliability, ease of implementation, and low computational costs, making it particularly suitable for wearable rehabilitation systems with limited resources. Furthermore, fixed angular limits ensure movement reproducibility and increase user safety by preventing deviations from physiologically acceptable ranges. Taken together, the laboratory test results confirm the functional viability of the L-CADEL v5 prototype and its potential for further use in assisted rehabilitation and elbow joint training.

A. Data from sensors

Figures 6, 7, and 8 show real-time visualizations of data from the sensors, implemented through the developed web interface of the L-CADEL v5 prototype. The system architecture is built on a client-server model: a microcontroller integrated into the control unit collects data from the IMU sensor and DYNAMIXEL servomotors, then transmits it wirelessly (Wi-Fi) to the server application via the secure WebSocket protocol (SSL). Data is transmitted in JSON format, ensuring structured data and compatibility with web technologies.

Figure 6 shows the dynamics of forearm orientation angles—Pitch (red line) and Roll (green line). The coordinate system corresponds to that introduced previously in Fig. 5: Pitch is rotation around the Y-axis and reflects movement in the sagittal plane (elbow flexion–extension). At the same time, Roll is rotation around the X-axis and characterizes lateral deviations of the forearm. The figure represents the execution of three consecutive elbow flexion–extension cycles during a single exercise at a natural speed of 30 seconds per cycle. The IMU sampling frequency is approximately 100 Hz; signal filtering was not applied in this series of experiments, which allows one to evaluate the "raw" measurement dynamics and the level of the noise component. Angle calculations are performed in real time via the web interface using standard trigonometric transformations, reducing the computational load on the microcontroller and increasing the system's scalability.

The pitch profile shows the expected monotonic dynamics during flexion and extension, confirming the correctness of the motion recording. The pitch angle is calculated based on the acceleration components using the formula:

$$Pitch = atan2\left(\frac{ax}{\sqrt{ax^2 + az^2}}\right) \quad (1)$$

Where, *ax*, *ay*, *az* are the acceleration components of the accelerometer attached to the user's wrist. During the experiment, pitch angle values ranged from 186.56° to 106.90°, within the physiologically acceptable range of motion under the specified protocol conditions.

At the same time, the roll analysis reveals small lateral deviations, indicating incomplete isolation of motion in this plane. The roll angle is calculated using the expression:

$$Roll = atan2\left(\frac{-ax}{\sqrt{ay^2 + az^2}}\right) \quad (2)$$

Theoretically, with ideal exercise performance, movement should occur predominantly in the sagittal plane, and the roll values should remain virtually constant. However, experimentally recorded tilt variations ranging from 195.20° to 208.89°, indicating lateral displacement of the forearm during exercise. These deviations may be due to individual motor control characteristics, compensatory movements of the shoulder joint, or mi-cro-movements of the sensor mount.

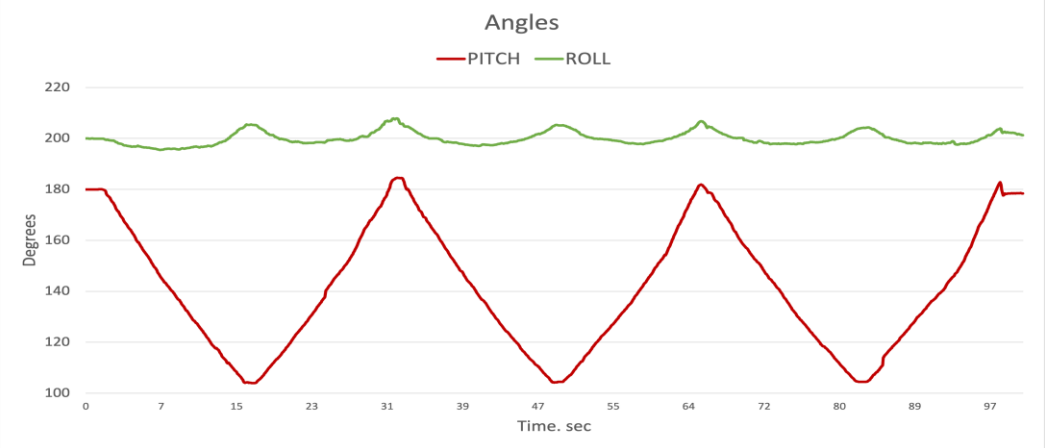

Fig. 6. Acquired data during a test with L-CADEL.v5 prototype in terms of Pitch and Roll angles.

Figure 7 shows the IMU acceleration components during three consecutive flexion-extension cycles. Thus, analysis of the acceleration components allows us to characterize further the movement's dynamics, including its smoothness, phase symmetry, and the presence of micromovements. The *Ax* and *Az* components correspond to accelerations in the sagittal plane in the horizontal and vertical directions, respectively. Signal analysis reveals that the greatest oscillation amplitude is observed along the *Ax* axis, corresponding to the horizontal direction in the sagittal plane.

This component is most sensitive to the flexion and extension phases of the elbow joint and exhibits pronounced periodic extremes synchronized with the change in direction of movement. In contrast, the *Ay* component is characterized by a smaller amplitude of value variations. The (Ax) values range from 0 to 9.88 m/s², while the *Az* values range from 2.33 to 8.98 m/s². These ranges are consistent with cyclic changes in the spatial orientation of the forearm and reflect periodic variations in the horizontal and vertical components of acceleration during rotational motion. The repeatability of the signal shape over three consecutive cycles indicates a stable kinematic profile of the movement. The *Ay* component exhibits a less stable pattern, varying between 2.34 and 4.12 m/s². The presence of values along this axis indicates that forearm movement is not completely constrained by the sagittal plane and is accompanied by lateral deviations of the wrist. Factors influencing the signal structure may include micro-movements of the sensor mount, changes in the tension of the connecting cables, or signs of user muscle fatigue, which can lead to changes in the movement trajectory.

To assess the integral intensity of movement, the magnitude of the acceleration vector was calculated (formula 3). This parameter allows estimating the total dynamic load regardless of sensor orientation and can be used for subsequent analysis of movement energy characteristics and for identifying anomalies in the kinematic profile. The graph shows that the modulus remains within a relatively narrow range (approximately 8.8–10.2 m/s²) and exhibits weak periodic oscillations synchronized with flexion–extension cycles.

$$|a| = \sqrt{ax^2 + ay^2 + az^2} \tag{3}$$

where *ax*, *ay*, *az* are the acceleration components of the IMU accelerometer attached to the wrist. Small wave-like changes in the modulus reflect the dynamic component of the motion, but their amplitude is small, indicating a smooth, controlled motion. The repeatability of the curve shape over three cycles indicates a stable kinematic profile and the coordinated operation of the servo drives and control algorithm. Overall, the modulus curve confirms that the motion is performed rhythmically, with moderate dynamic load and high repeatability between cycles.

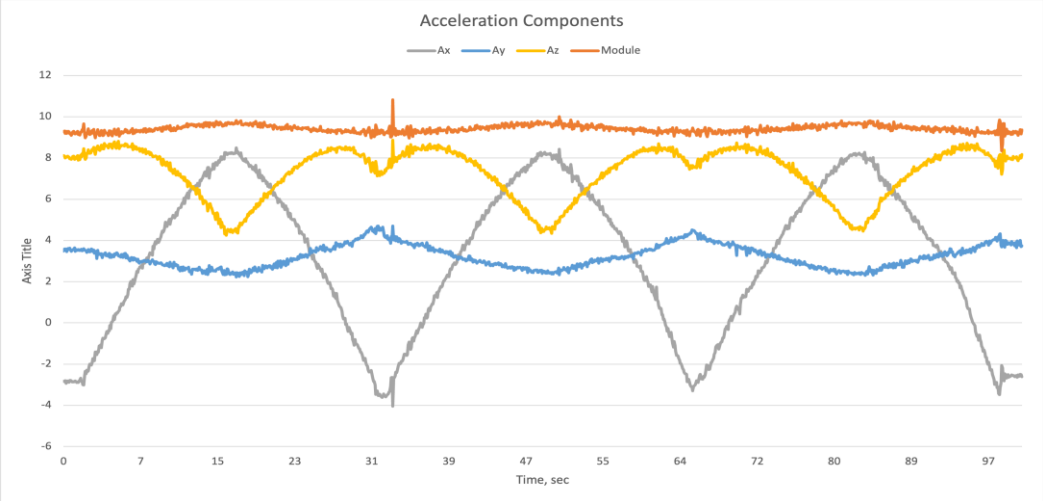

Fig. 7. Acquired data during a test with L-CADEL.v5 prototype in terms of acceleration components *Ax*, *Ay*, *Az* and Module.

Figure 8 shows the time dependence of angular velocity recorded by the IMU MPU-6050, installed on the user's wrist. The figure reflects gyroscope data along two axes: *Gx* (blue line) and *Gz* (gray line)—during three consecutive elbow flexion-extension cycles. The *Gx* component demonstrates the most pronounced dynamics and corresponds to the main plane of motion (sagittal). Positive angular velocity values are recorded during the flexion phases, while negative ones are recorded during the extension phases, reflecting a change in the direction of forearm rotation relative to the elbow joint. The angular velocity amplitude is ±4 to ±10 °/s, corresponding to a controlled, moderate tempo of exercise performance. At moments of direction reversal (the transition from flexion to extension and vice versa), short-term extremes are observed, reaching higher absolute values. These peaks are due to inertial effects, the instantaneous reversal of the angular velocity, and the dynamic response of the servo drive control system. The *Gz* component has a significantly lower amplitude and fluctuates near zero. This indicates that the movement occurs predominantly in one plane, with rotation around the *Z*-axis being secondary. Minor deviations may be due to micro-movements of the shoulder joint, imperfect sensor fixation, or individual user characteristics. The absence of significant oscillations along the *Z*-axis confirms the correct execution of the exercise and the relative isolation of movement in the sagittal plane.

The signal structure is consistent across all three cycles, indicating the reproducibility of the kinematic profile and the stability of the control algorithm. The observed noise level is typical for the MPU-6050 gyroscope without additional digital filtering. Overall, the obtained data confirm that the MPU-6050 provides adequate angular velocity recording for elbow motion monitoring and can be effectively used to analyze the dynamic characteristics of the exercise.

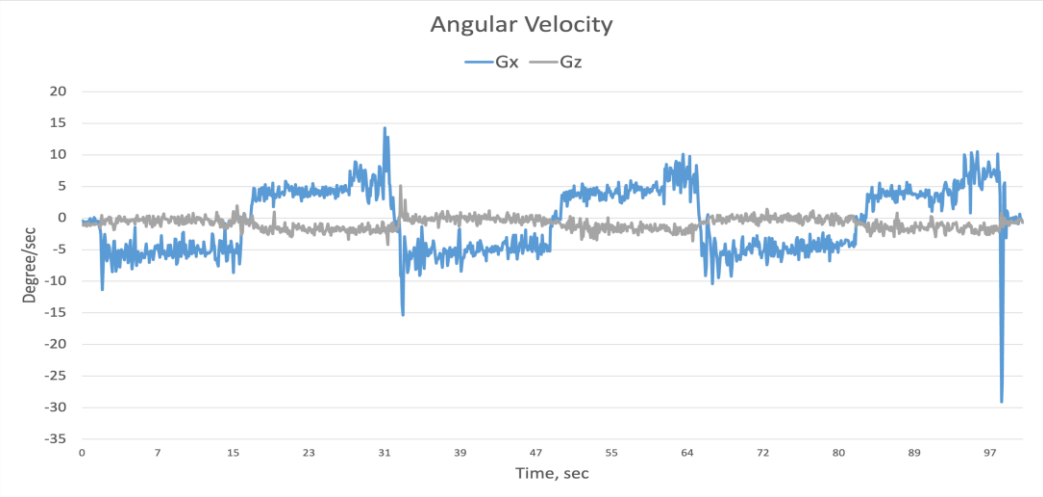

Fig. 8. Acquired data during a test with L-CADEL.v5 prototype in terms of angular velocity *Gx*, *Gz*.

Table 2 shows the maximum and minimum parameter values recorded by the L-CADEL v5 prototype sensor system during experimental testing. The presented ranges reflect the amplitude characteristics of angular positions and acceleration components. The stability of the values between cycles indicates the reproducibility of the results and the robustness of the system. Taken together, the presented data confirm that L-CADEL v5 meets its stated functional characteristics and can be considered a promising platform for assisted rehabilitation and upper-limb movement monitoring.

TABLE 2
RESULTS OF THE MAXIMUM AND MINIMUM VALUES WITH L-CADEL V.5 PROTOTYPE, DATA FROM SENSORS

Components	Max	Min
Pitch (deg)	186	106
Roll (deg)	206	195
Acceleration components Ax (m/s^2)	8.56	-2.88
Acceleration components Ay (m/s^2)	4.21	-0.23
Acceleration components Az (m/s^2)	9.45	4.24
Module (m/s^2)	10.56	9.11
Angular velocity Gx (deg/s)	4.21	-0.23
Angular velocity Gz (deg/s)	9.45	4.24

B. Kinovea software

Fig. 9 shows a volunteer during experimental testing at the IPN Laboratory. The volunteer was seated, with the forearm resting on a horizontal tabletop. This position minimizes unwanted shoulder and trunk movements. During the experiment, the volunteer performed three flexion-extension cycles at a natural speed of around 30 seconds per cycle. For motion analysis using Kinovea software, a system of five reference markers is placed on anatomical landmarks and device elements.

Markers highlighted in green (markers 1, 2, 3) were used to determine the anatomical elbow joint angle formed by the shoulder-elbow-wrist segments. This configuration allows for the calculation of the true biomechanical elbow flexion/extension angle, independent of the assistive device design. Additionally, markers highlighted in red (4, 2, 5) were used to record the functional angle between the device elements, as determined by the Arm Platform-elbow-Wrist Platform configuration. This angle characterizes the kinematics of the assistive mechanism itself and reflects the motion generated by the servo drives and cable system. In the Kinovea software, both angles were analyzed synchronously, allowing comparison of their temporal dynamics, amplitude characteristics, and the consistency between the user's anatomical motion and the device's mechanical motion. This approach provides a comprehensive assessment of the accuracy, efficiency and biomechanical correctness of the L-CADEL v5 system.

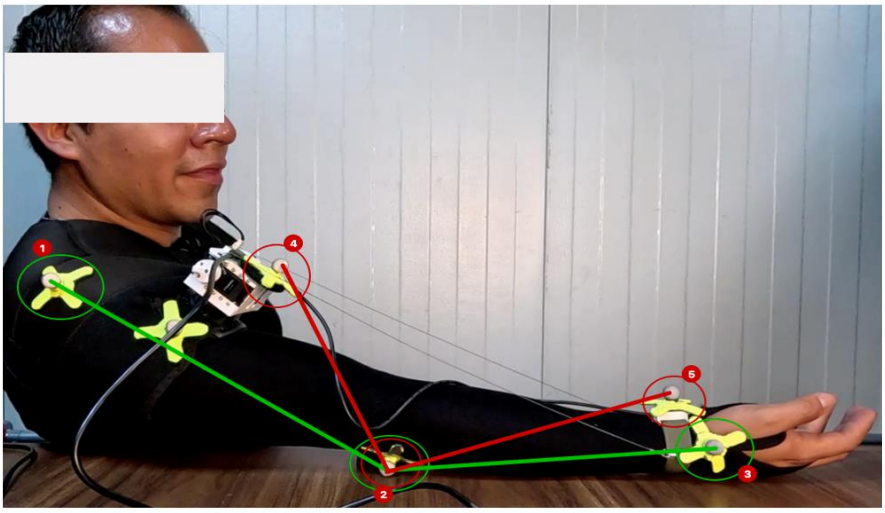

Fig. 9. L-CADEL v5 with markers attached to the volunteer: (1, 2, 3) Biomechanical angle; (4, 2, 5) Device angle.

The sequence of five screenshots shown in Fig. 10 illustrates the process of one elbow flexion-extension cycle performed by volunteer ID M.3 with the L-CADEL v5 assistive device installed. The experiment was conducted in a laboratory setting with a standardized posture: the subject was seated, with the forearm resting on the table. The volunteer performed three elbow flexion-extension cycles with a natural speed of 30 seconds per cycle. The initial phase of the movement is shown in Fig. 10(a), where the table fully supports the forearm and the hand is in a supinated position, forming a zero angular position. The lifting phase (Fig. 10 (b)) is characterized by elbow flexion to approximately 45°, accompanied by slight wrist rotation. The maximum flexion phase is shown in Fig. 10 (c), where the forearm assumes a nearly vertical position. Next comes the controlled extension phase (Fig. 10 (d)), during which the forearm is smoothly lowered. The final phase (Fig. 10 (e)) is the return to the starting position with support on the table, completing the full cycle of movement.

Kinematic analysis was performed using Kinovea software, which calculated two independent angular trajectories. The first trajectory (green curve) corresponded to the anatomical angle defined between the "wrist - elbow - shoulder" vector and reflected a biomechanical assessment of upper limb movement. The second trajectory (blue curve) represented the angle between the "Wrist Platform - elbow - Arm Platform" vector and characterized the kinematics recorded directly by the L-CADEL v5 device. Comparison of these angles allows us to evaluate the consistency between anatomical movement and the device's mechanical response, identify possible differences in amplitude, and assess potential platform displacements relative to anatomical landmarks.

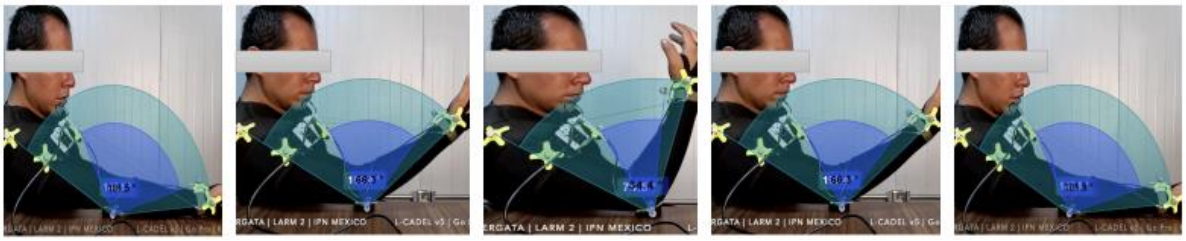

Fig. 10. Snapshots of flexion-extension exercise by a volunteer for elbow testing device L-CADEL v5 with Kinovea analysis.

Based on the coordinates of the reference markers extracted from the video recordings, two independent elbow flexion angles were calculated for each frame. The first angle corresponds to the "anatomical angle" defined by the "wrist-elbow-shoulder" segments and reflects the biomechanical position of the upper limb. The second angle characterizes the "device angle" and is formed by the "Wrist Platform-elbow-Arm Platform" segments, describing the movement kinematics recorded directly by the L-CADEL v5 system. In both cases, the center of measurement was the marker located in the elbow joint, while the wrist vector and shoulder vector differed depending on the selected marker configuration.

Figure 11 shows three consecutive elbow flexion-extension cycles performed using the L-CADEL v5 prototype. Each cycle demonstrates a distinct phase transition from the maximum angular value corresponding to the extension phase to the minimum value during the flexion phase, followed by a return to the initial position. The time profiles of both angular trajectories demonstrate a high degree of synchrony and phase coincidence, indicating coordinated motion between the anatomical markers and the device elements. At the same time, the absolute values of the "anatomical angle" systematically exceed the "device angle" values. This discrepancy is explained by the spatial location of the anatomical shoulder marker, which is somewhat proximal to the Arm Platform marker, forming a more open geometric angle. As a result, the anatomical angle varies over approximately 78–156 deg, while the angle measured by the device

exhibits a more compact range—54–132 deg. Despite this, the difference between the two signals remains stable throughout all three cycles, and both curves demonstrate high reproducibility, periodicity, and temporal consistency. These results confirm the correctness of motion capture, the stability of the angle calculation algorithm, and the reliability of the L-CADEL v5 system in dynamic analysis of elbow joint movements.

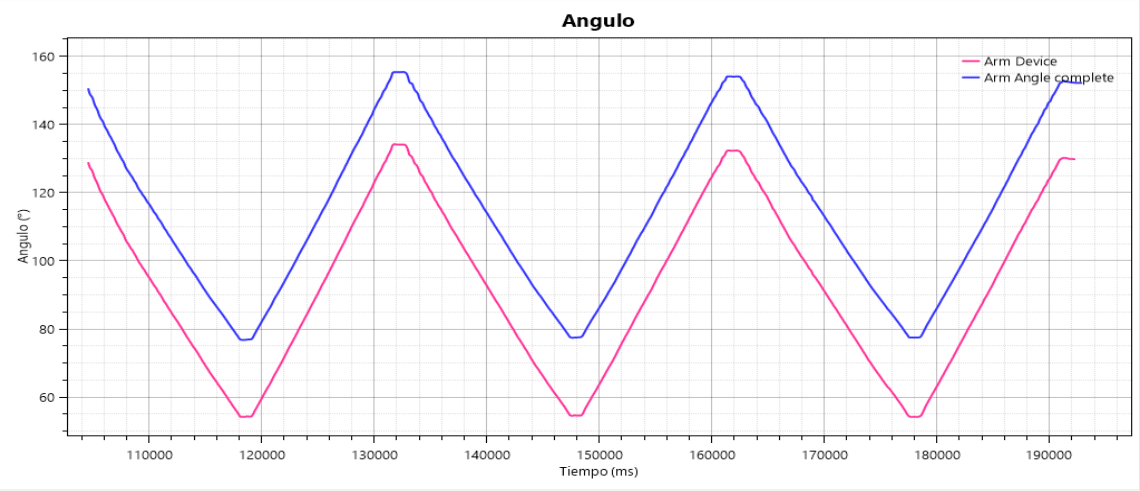

Fig. 11. Analysis of the Kinovea software of test with the L-CADEL.v5 prototype in terms of Pitch angle: Anatomical and Device angles.

Calculations were performed in the image plane (2D), which corresponds to the Kinovea methodology. For each video frame, the two-dimensional coordinates of the markers are known:

$$W = (x_W, y_W),\ E = (x_E, y_E),\ S = (x_S, y_S),\ WP = (x_{WP}, y_{WP}),\ AP = (x_{AP}, y_{AP}) \quad (4)$$

Where, *W* is the wrist, E is the elbow, *S* is the shoulder, *AP* is the Arm platform, *WP* is the Wrist platform markers. The first step is to construct vectors. Both angles share a common center—the ulnar marker *E*. Therefore, two sets of vectors are formed:

"Anatomical angle":

$$V_1 = \overline{EW} = (x_W - x_E, y_W - y_E),\ V_2 = \overline{ES} = (x_S - x_E, y_S - y_E) \quad (5)$$

"Device angle":

$$V_3 = \overline{EWP} = (x_{WP} - x_E, y_{WP} - y_E),\ V_4 = \overline{EAP} = (x_{AP} - x_E, y_{AP} - y_E) \quad (6)$$

The next step is to calculate the dot product and the vector norms. The dot product is calculated using the formula:

$$V_1 \cdot V_2 = v_{1x}\, v_{2x} + v_{1y} v_{2y},\ \ V_3 \cdot V_4 = v_{3x}\, v_{4x} + v_{3y} v_{4y} \quad (7)$$

The final step is to calculate the angles using the dot product:

$$\theta_{Anatomical\ angle} = arccos\left(\frac{V_1 \cdot V_2}{\|V_1\|\|V_2\|}\right), \quad \theta_{Device\ angle} = arccos\left(\frac{V_3 \cdot V_4}{\|V_3\|\|V_4\|}\right) \tag{8}$$

Figure 12 shows two time series of elbow joint angular velocity calculated based on the derivative of angular positions. Both time series exhibit three distinct phase transitions corresponding to three cycles of elbow flexion/extension. During the dynamic flexion and extension phases, distinct positive and negative peaks in angular velocity are recorded. In this configuration, positive peaks correspond to the elbow extension phase, while negative peaks are associated with the flexion phase. This signal structure is consistent with the expected biomechanics of the movement and confirms the correctness of the calculations of the angular trajectory derivatives. A comparative analysis of the two curves shows that the angular velocities are almost completely synchronous in time, including the moments of reaching extreme values and changing direction. This demonstrates high temporal consistency of the angles. The figure shows that the "anatomical angle" consistently exhibits slightly higher peak angular velocity and smoother peak shapes than the "device angle." The "device angle" data exhibit lower peak amplitudes, which may be due to differences in marker placement geometry. These results confirm the reproducibility of the kinematic characteristics of the movement and demonstrate that the L-CADEL v5 system provides adequate and stable recording of elbow joint dynamics during rehabilitation exercises.

Angular velocity is calculated as the discrete first derivative of the joint's angular position. For frame k, the angular velocity is determined using the formula:

$$w_k = \frac{\theta_k - \theta_{k-1}}{\Delta t} \tag{9}$$

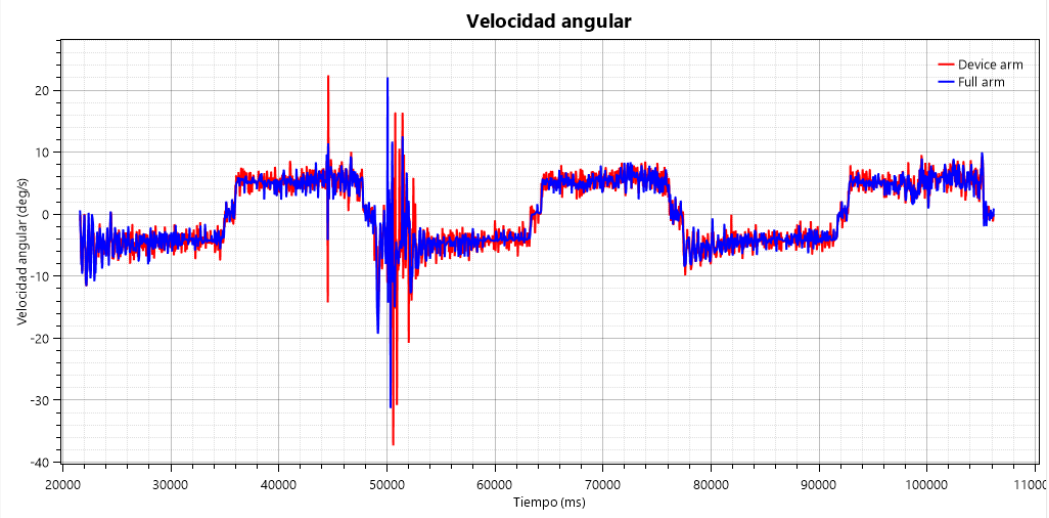

Fig. 12. Analysis of the Kinovea software of test with the L-CADEL.v5 prototype in terms of Angular Velocity: Anatomical angle and Device angle.

Figure 13 shows the time series of elbow joint angular acceleration calculated as the second derivative of angular position based on previously calculated angular velocities for two measurement configurations: "anatomical angle" and "device angle". Both signals are characterized by a high level of high-frequency noise, which is expected, since angular acceleration is the second derivative with respect to time of angular position and, therefore, amplifies the influence of video tracking errors, time-scale quantization, and marker microshifts. In intervals corresponding to static arm holding or quasi-stationary phases of movement, the angular acceleration values oscillate around zero, forming a nearly horizontal noise background without pronounced peaks, indicating the absence of active rotational acceleration in the elbow joint. During the dynamic flexion and extension phases, pronounced positive and negative peaks in angular acceleration are observed. Both curves exhibit a similar temporal structure and value synchrony, indicating consistent kinematic characteristics. Minor differences in amplitude may be due to geometric differences in the placement of the anatomical shoulder marker and the device marker, as well as local filtering effects and the accumulation of differentiation errors. Overall, the obtained results confirm that the L-CADEL v5 system accurately records elbow joint motion dynamics.

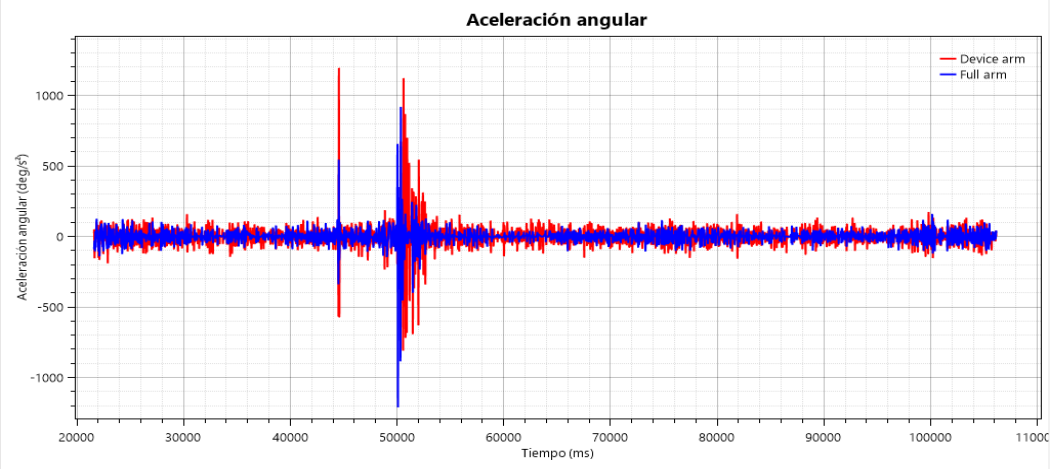

Fig. 13. Analysis of the Kinovea software of test with the L-CADEL.v5 prototype in terms of Angular Acceleration: Anatomical angle and Device angle.

Figure 14 shows the linear velocity time series calculated from the angular trajectories obtained using the "anatomical angle" and "device angle" marker configurations. The figure displays three repeating clusters of velocity increases/decreases, each corresponding to one complete elbow flexion–extension cycle. The structure of each cluster is stable and includes a sharp increase in velocity, reflecting the onset of the active phase of the movement, followed by a decrease in velocity corresponding to the flexion phase, with the minimum velocity recorded at full flexion. This is followed by a smooth increase in velocity, indicating the extension phase. The maximum velocity values for both angles are recorded at full arm extension. Periodically, the "device angle" values exhibit more noise and fluctuations compared to the "anatomical angle" data. This may indicate the influence of micro-movements of the L-CADEL v5 prototype parts installed on the user's arm. A comparative analysis of three consecutive flexion-extension cycles reveals a similar phase and cyclic structure of movement. The high repeatability of peak shape and amplitude across cycles confirms the stability of the movement kinematics and the reliability of this measurement method.

Científica, vol. 30, no. 1, pp. 01-28, January-June 2026,
ISSN 2594-2921, Instituto Politécnico Nacional, México
e300106 | DOI: 10.46842/ipn.cien.v30n1a06

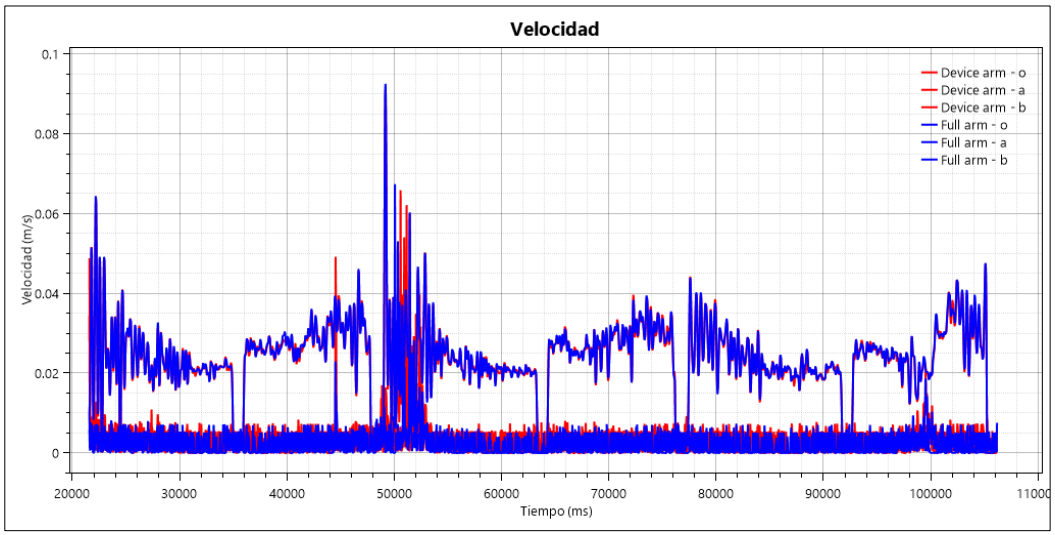

Fig. 14. Analysis of the Kinovea of the test with the L-CADEL.v5 prototype in terms of Velocity: Anatomical angle and Device angle.

Table 3 presents the minimum and maximum values of the kinematic parameters obtained through video kinematic analysis using Kinovea software. These data were calculated based on video recordings obtained during the experimental testing of the L-CADEL v5 device and reflect the maximum values of the measured parameters during elbow flexion and extension exercises.

TABLE 3
RESULTS OF THE MAXIMUM AND MINIMUM VALUES WITH L-CADEL V.5 PROTOTYPE: KINOVEA

Components	Max	Min
Anatomical angle (degree)	158	78
Device angle (degree)	132	54
Angular velocity of Anatomical angle (deg/sec)	10	-11
Angular velocity of Device angle (deg/sec)	10	-11
Angular acceleration of the anatomical angle (deg/sec2)	195	-168
Angular acceleration of Device angle (deg/sec2)	186	-156
Velocity of Anatomical angle (m/s)	0.08	0
Velocity of Device angle (m/s)	0.06	0

C. AI-based system

To analyze the elbow flexion/extension exercise using the L-CADEL v5 prototype, an AI-based video analysis system was additionally employed. A platform focused primarily on sports biomechanics is used, enabling automated processing of high-quality video streams up to 4K resolution at 120 fps. The system is based on computer vision and deep learning algorithms trained on extensive datasets of annotated human body images. During the processing stage, a pose estimation model automatically identifies key anatomical landmarks (keypoints)—the shoulder, elbow, wrist, and additional upper-limb segments. This study analyzed elbow flexion/extension movements of one arm. The

algorithms use convolutional neural networks (CNNs) to localize joints in each frame, followed by temporal filtering of the trajectories to improve coordinate stability. This results in a sequence of joint coordinates over time, which is used to calculate angular motion parameters.

Figure 15 presents a sequence of five screenshots illustrating one complete cycle of the elbow flexion-extension exercise. Figure 15(a) shows the starting position: the forearm is placed on the table surface, and the elbow joint is in full extension, corresponding to the initial and final positions of the movement. Figure 15(b) depicts the intermediate phase of flexion, during which the forearm is raised upward, and the elbow angle decreases by approximately 45° relative to the starting position, demonstrating a controlled movement. Figure 15(c) captures the phase of full flexion: the forearm is as close as possible to the shoulder, which corresponds to the minimum value of the joint angle in this cycle. Next, Figure 15(d) shows the intermediate phase of extension, reflecting the gradual return of the limb to the starting position. Figure 15(e) demonstrates the completion of the cycle—full extension of the elbow joint with the forearm returning to the table surface. This series of images sequentially reflects the kinematic structure of one cycle.

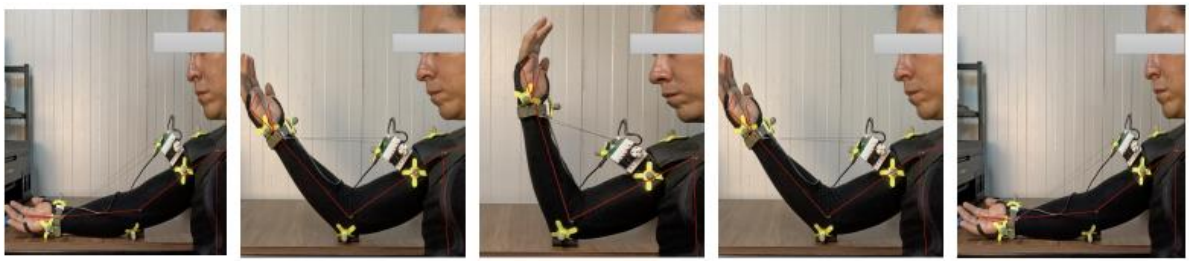

Fig. 15. Snapshots of flexion-extension exercise by a volunteer for the elbow testing device L-CADEL v5 with AI analysis.

Figure 16 illustrates the comparative analysis of 2D and 3D elbow joint angles (pitch component) recorded during three consecutive cycles of elbow flexion–extension. The horizontal axis represents time (s), while the vertical axis shows the elbow angle in degrees. The blue curve corresponds to the 2D angle obtained from planar pose estimation, and the orange curve represents the reconstructed 3D angle. The figure demonstrates a cyclic pattern characteristic of controlled flexion–extension movement. Across the three cycles, the 2D elbow angle varies approximately within the range of 95–185 deg, while the 3D angle fluctuates within a narrower corridor of 120–185 deg. Each cycle consists of a gradual decrease in angle (flexion phase), reaching a minimum near 95-100 deg (2D) and 120 deg (3D), followed by a progressive increase toward full extension, approaching 180–185 deg (2D) and 180–185 deg (3D). The periodicity and repeatability of the cycles indicate consistent execution of the exercise. A large amount of noise can be seen in the figure, especially in the area of maximum elbow extension. This effect is mainly due to the AI-based pose estimation system's automatic placement and tracking of virtual markers. The use of monochrome clothing, such as OptiTrack, makes it more difficult for the AI algorithm to determine joint positions accurately. Therefore, at near-full elbow extension, the system has the greatest difficulty determining the correct position of the elbow marker. Therefore, the figure shows significant noise at full extension. After the movement transitions from full extension to flexion, the angle increases, improving geometric stability and reducing sensitivity to small coordinate deviations; consequently, the noise amplitude decreases.

Comparing the two datasets, the 2D angle appears more physiologically realistic in terms of range of motion. The 2D data demonstrate a wider, more anatomically consistent range of motion during elbow flexion and extension under the testing conditions. In contrast, the 3D reconstruction shows a systematically reduced dynamic range. This difference may be due to uncertainty in depth estimation in monocular 3D reconstruction, limitations in the AI model's smoothing,

and regularization methods that stabilize spatial key points at the expense of amplitude accuracy. Thus, with controlled motion in the sagittal plane and a fixed camera orientation, 2D analysis can provide a more direct, geometrically transparent assessment of joint angle.

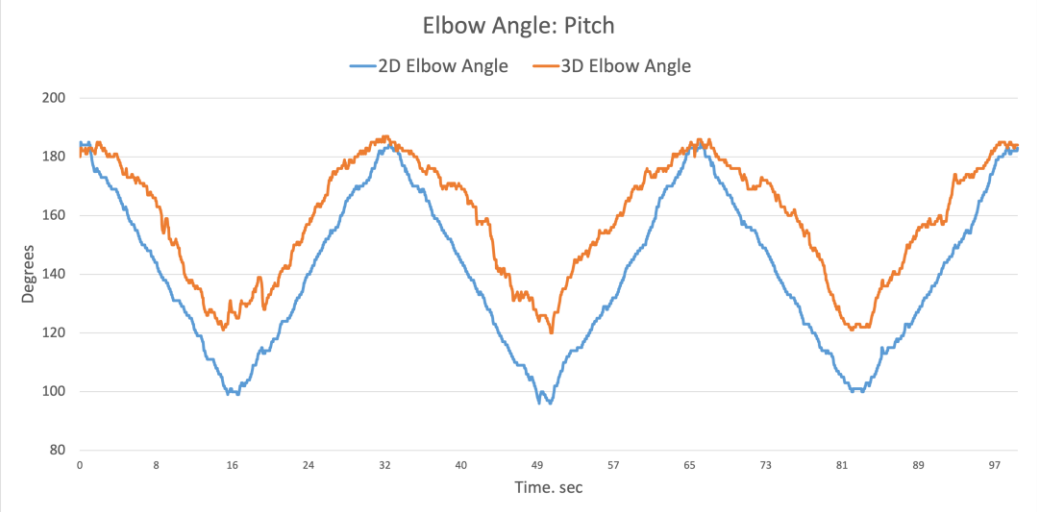

Fig. 16. Analysis of the AI of test with the L-CADEL.v5 prototype in terms of Pitch angle: 2D interpretation and 3D interpretation.

In 2D mode, the system calculates angles in the image plane based on joint coordinates defined in the frame's pixel coordinate system. For the elbow joint, the angle between the shoulder-elbow and elbow-wrist segments is determined using the vector product. This approach allows one to determine the flexion angle in the sagittal plane. The accuracy of the 2D method depends on camera position, distortion, and scale calibration. The elbow joint angle is calculated using the dot product formula:

$$\theta = arccos\left(\frac{\vec{u}\,.\vec{v}}{|\vec{u}|.\,|\vec{v}|}\right) \tag{10}$$

Where Shoulder: $S(x_s, y_s)$, Elbow: $E(x_e, y_e)$, Wrist: $W(x_w, y_w)$, and the vectors are calculated using the formula:

$$\vec{u} = S - E = (x_s - x_e, y_s - y_e), \quad \vec{v} = W - E = (x_w - x_e, y_w - y_e) \tag{11}$$

In 3D mode, the system reconstructs the spatial coordinates of joints either via stereoscopic reconstruction (using multiple cameras) or via depth reconstruction models trained to estimate depth from a single video stream. The angle between segments is calculated similarly in 3D. In this case, each point corresponds to a coordinate vector of $S(x_s, y_s, z_s)$, $E(x_e, y_e, z_e)$, $W(x_w, y_w, z_w)$. Thus, using an AI video analysis system with the L-CADEL v5 prototype provides additional verification of kinematic parameters and increases the reliability of experimental results.

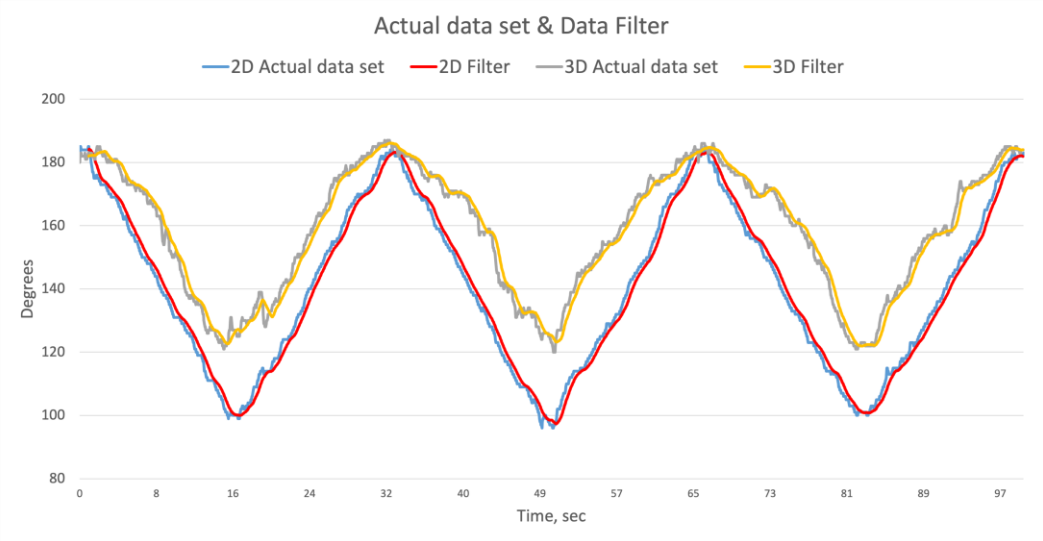

Fig. 17. Analysis of the AI of test with the L-CADEL.v5 prototype in terms of Pitch angle: 2D interpretation with Filter.

In Figure 17, a standard smoothing filter implemented in Microsoft Excel was applied to the 2D and 3D elbow angles data to reduce noise. For 2D angle, the figure shows two curves: the original signal (blue) and the filtered signal (red). The applied Filter attenuates rapid fluctuations while preserving the overall trend and periodic structure of the movement cycles. The noise reduction is particularly noticeable near the peaks corresponding to full extension, where marker instability previously caused sharp jumps. After filtering, the curve becomes smoother and the extremes more clearly defined, facilitating a more precise determination of the range, maximum, and minimum values. Thus, using a filter to smooth the signal increases the reliability of peak and range determination. It also improves comparability with data obtained from the L-CADEL v5 prototype or from motion analysis using Kinovea software.

TABLE 4
RESULTS OF THE MAXIMUM AND MINIMUM VALUES WITH L-CADEL V.5 PROTOTYPE: AI-BASED SYSTEM

Components	Max	Min
2D angle (degree)	185	95
3D angle (degree)	185	120
2D angle with Filter (degree)	183	98
3D angle with Filter (degree)	183	123

D. Range of Motion & Mean

The value range and average are calculated separately for each measurement method: L-CADEL v5 prototype sensors, video analysis in Kinovea, and the AI system. This ensures accurate data comparison. Generating a value range and an average trajectory allows for capturing a typical biomechanical movement profile and assessing exercise repeatability. In practical terms, this can improve the reliability of kinematic analysis and enable the resulting information to serve as a benchmark for subsequent exercise performance assessment or calibration of measurement systems.

The average value and a range of acceptable values are calculated in stages. In the first stage, the time scale is normalized—each recording of a single repetition is normalized to 100% of the cycle duration (0–100%), allowing accurate comparison across repetitions regardless of their actual duration. In the second stage, all obtained curves of the same type are superimposed on one another in a single coordinate system. In the next step, the min and max values are calculated for each moment, and the Average value is calculated according to the formula:

$$Arithmetic\ Mean = \frac{\sum_{i=1}^{n} Pitch_i}{n}, \qquad RMS\ Mean = \sqrt{\frac{1}{N}\sum Pitch_i^2} \tag{12}$$

Figure 18 shows the elbow flexion-extension angle profile obtained using the inertial measurement unit (IMU) of the sensor system. The *x*-axis represents the normalized movement time (% of cycle), and the *y*-axis represents the elbow angle (degrees). The movement involves repeated cycles of elbow flexion and extension.

The red line represents the arithmetic mean, while the blue line represents the root mean square (RMS). The light orange area displays the range of minimum and maximum angle values (MIN–MAX), characterizing the variability in measurements across movement cycles.

The resulting profile demonstrates a periodic pattern of angle change corresponding to successive cycles of elbow flexion and extension. Maximum angle values are observed at approximately 180-185°, corresponding to full extension, while minimum values are around 105-110° and correspond to the maximum flexion phase. The presence of multiple repeating cycles indicates stability in movement performance throughout the experiment. The high degree of agreement between the Arithmetic Mean and RMS Mean curves indicates a low level of deviation and the absence of significant outliers in the recorded data. Minor differences between the two parameters are observed primarily in regions of extreme angle values, which may be due to sensor noise, changes in movement speed, or small variations in limb position between cycles.

The width of the MIN-MAX region varies across movement phases: the range increases primarily in the transition regions between flexion and extension, which may indicate increased variability in the movement trajectory or greater sensitivity of the inertial sensor to dynamic changes in acceleration. Overall, the results demonstrate robust recording of elbow joint kinematic parameters by the sensor system and confirm the feasibility of using an inertial sensor for quantitative motion analysis during rehabilitation.

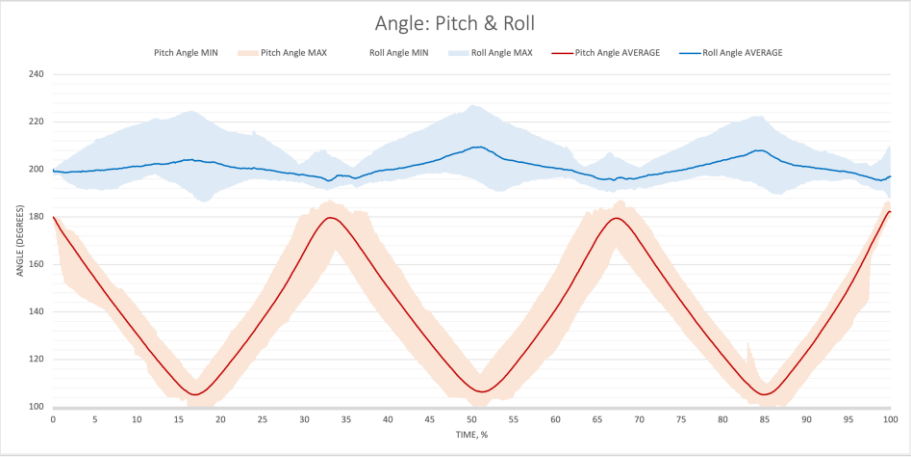

Fig. 18. Range of Motion and Mean from Sensors in terms of Pitch and Roll angles.

To further validate the sensor system data, additional elbow motion analysis was performed in Kinovea. Unlike the inertial approach, which relies on embedded sensors to record spatial orientation, video analysis enables the evaluation of kinematic motion parameters by tracking anatomical landmarks in the image. The use of Kinovea in this study aimed to obtain an independent set of measurements for comparison with the sensor system's results and to assess the consistency between different motion recording methods.

Figure 19 shows the elbow flexion-extension angle profile obtained using video analysis. The *x*-axis represents the normalized movement execution time (% of cycle), and the y-axis represents the angle of motion in degrees. The analysis includes several consecutive cycles of elbow flexion and extension.

The red curve represents the device average angle, while the blue curve corresponds to the arm average angle, determined from the positions of anatomical landmarks during video processing. The light orange and light blue areas represent the minimum and maximum values (MIN-MAX), reflecting the variability in measurements across repeated movement cycles.

The obtained results demonstrate a consistent periodic pattern of angular parameter changes corresponding to repeated cycles of elbow flexion and extension. The signal shape shows high repeatability across individual cycles, indicating the stability of movement performance and the reproducibility of measurement results.

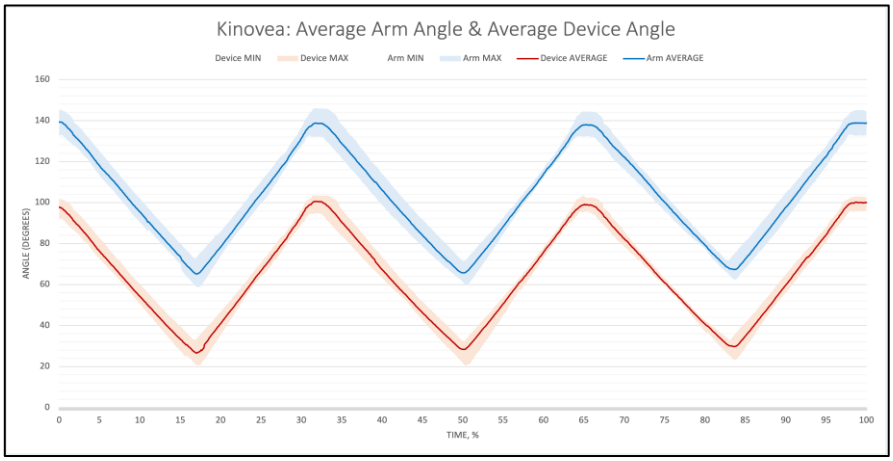

Fig. 19. Range of Motion and Mean from Kinovea software analysis in terms of Pitch angle: Anatomical angle and Device angle.

As the next step in the comparative analysis, an AI-based computer vision system was used to automatically locate joint points and calculate angular motion parameters without the use of physical markers. Unlike the sensor-based approach and semiautomated video analysis in Kinovea, this method provides fully automated data processing and allows simultaneous motion assessment in both 2D and 3D. However, in this study, the primary focus was on 2D angle analysis, as this approach demonstrated higher stability of results and better matched the comparison conditions with data obtained from the Kinovea sensor system and video analysis.

The red curve represents the average angle calculated in 2D space (2D Angle Average), and the blue curve represents the average angle in 3D space (3D Angle Average). The light orange and light blue areas represent the minimum and maximum ranges (MIN–MAX) for each measurement method.

The results demonstrate a pronounced periodic signal structure corresponding to repeated cycles of elbow flexion and extension. 2D analysis reveals a clearly defined motion profile with successive maxima and minima reflecting the transition between the flexion and extension phases. Maximum 2D angle values are approximately 150–160°, while minimum values are around 75–80°. The curve shape shows high repeatability across cycles, indicating the stability of the motion recording.

Overall, the AI-based analysis results confirm the feasibility of automatically tracking elbow joint kinematics without the use of physical markers.

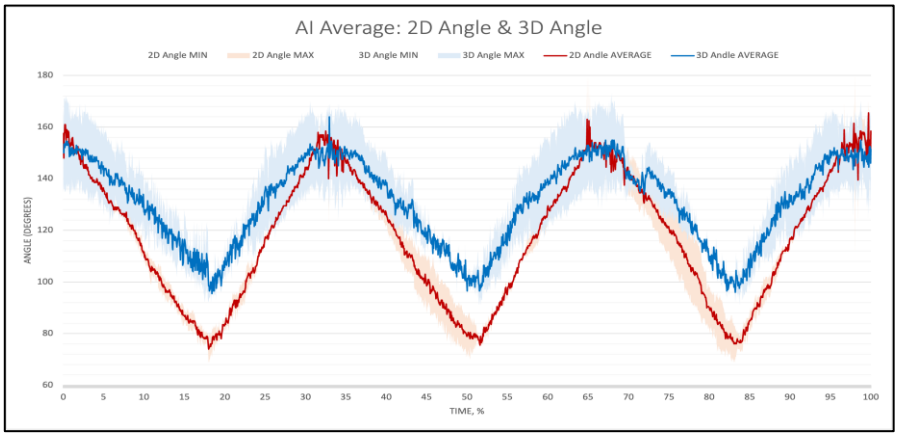

Fig. 20. Range of Motion and Mean form AI-based system in terms of Pitch angle: 2D interpretation and 3D interpretation.

The results showed that all three methods successfully captured repeated elbow flexion-extension cycles and demonstrated similar dynamics of angular parameter changes.

The IMU-based sensor system demonstrated stable real-time motion recording with low cycle-to-cycle variability, confirming the reliability of inertial sensors for monitoring rehabilitation exercises. An additional advantage of this approach is its autonomy, independence from external cameras, and the ability to be used in a home rehabilitation setting.

Video analysis using Kinovea yielded highly repeatable results and enabled reproducible assessment of motion kinematics. Despite the need for manual or semiautomated landmark determination, this method can serve as an accessible tool for comparative evaluation and data validation.

The AI-based motion analysis system provided fully automated data processing and the ability to determine motion parameters without the use of physical markers. The results showed that two-dimensional (2D) analysis was characterized by greater stability and less variability than three-dimensional (3D) analysis, making it more suitable for comparison with sensory system and video analysis results.

Despite differences in absolute angle values, all methods demonstrated a high degree of similarity in the shape of the kinematic profiles and the sequence of movement changes. Thus, the obtained results confirm the potential of L-CADEL v5 as a compact, portable, and cost-effective solution for performing elbow exercises.

IV. Conclusions

This study conducted a comprehensive evaluation of the L-CADEL v5 prototype during flexion-extension exercises. The comparative analysis included three independent measurement methods: sensor data, video analysis in Kinovea software, and an AI system. The sensor data demonstrated high stability and clearly defined cyclic dynamics corresponding to the flexion and extension phases of the elbow joint. Analysis of multiple datasets revealed a narrow range of values, indicating good repeatability of the movement and reliability of sensory registration. Calculation of the pitch angle from acceleration components showed that the device adequately reflects the primary plane of forearm motion. Video analysis in Kinovea demonstrated good agreement between the dynamics, the range of values, and the sensor data. The synchronicity of the extremes, the similarity of the amplitude, and the shape of the averaged curves confirm the correct installation of the prototype on the user's hand and minimal platform displacement during the exercise. This also demonstrates the mechanical stability of the structure and its compliance with anatomical kinematics. The consistency between the sensor data and Kinovea data provides confirmation of the prototype's validity and the appropriateness of the chosen measurement method. The AI system demonstrated the ability to correctly identify movement phases and reproduce the signal's overall cyclical structure. Despite a somewhat wider range of variability and increased noise, particularly in the 3D reconstruction, the averaged curves retained a physiologically relevant shape and were in phase with the sensory and video data. The higher variability in the AI data may be due to the specific algorithms used to detect joint points automatically.

Nevertheless, the obtained data confirm that AI analysis can be used as an additional tool for movement assessment. Of particular importance is the analysis of averaged data from more than 100 volunteers. The comparability of the dynamics and value ranges between the methods confirms the robustness and reproducibility of the prototype across a broad user population.

Thus, the L-CADEL v5 prototype demonstrated satisfactory accuracy, stability, and consistency with independent analysis methods. The device can be considered a promising tool for objectively assessing elbow joint motion, monitoring exercise technique, and for use in rehabilitation and sports programs. The obtained results confirm the feasibility of further development and implementation of the system in biomechanical analysis.

CRediT (*Contributor Roles Taxonomy*)

Author Contributions: Conceptualization, M**C** and S**K**; methodology, M**C**.; software, S**K**; validation, M**C** and S**K**; formal analysis, M**C** and S**K**; investigation, M**C**. and S**K**; resources, M**C**.; data curation, S**K**; writing—original draft preparation, M**C**. and S**K**; writing—review and editing, M**C**. and S**K**; visualization, S**K**; supervision, M**C**; project administration, M**C**; funding acquisition, M**C**. All authors have read and agreed to the published version of the manuscript.

Institutional Review Board Statement: The study was conducted in accordance with the Declaration of Helsinki and was approved by the Institutional Ethics Committee of the Policlinico di Tor Vergata, Rome, under protocol code RS. 197.22 on November 15, 2022.

Informed Consent Statement: Informed consent was obtained from all subjects involved in the study.

Data Availability Statement: data is unavailable due to privacy restrictions linked to the volunteer of the testing activity.

Acknowledgments: The first author like to acknowledge the team of the SEPI-ESIME-Zacatenco of the National Polytechnic Institute in Mexico City for hosting him during a semester in 2025-2026 and providing frames for testing campaign. This is to acknowledge PhD scholarship funded by the DM118 program of the Italian Ministry for Research.

Conflicts of Interest: The authors declare no conflicts of interest.

REFERENCIAS

[1] R. D. Zorowitz, R. Harvey, J. Stein, C. Winstein, G. Wittenberg, *Stroke Recovery and Rehabilitation*. New York, NY, USA: Demos Medical Publishing, 2014.
[2] J. Kacprzyk, V. E. Balas, M. Ezziyyani, Eds., *Advanced Intelligent Systems for Sustainable Development (AI2SD'2020)*, vol. 1417. Cham, Switzerland: Springer, 2022, doi: https://doi.org/10.1007/978-3-030-90633-7
[3] A. Alamdari, V. Krovi, "Robotic Physical Exercise and System (ROPES): A cable-driven robotic rehabilitation system for lower-extremity motor therapy," in *Proc. ASME 39th Mech. Robot. Conf.*, 2015, Art. no. V05AT08A032, doi: https://doi.org/10.1115/DETC2015-46393
[4] M. Ceccarelli, L. Ferrara, V. Petuya, "Design of a cable-driven device for elbow rehabilitation and exercise," in *Interdisciplinary Applications of Kinematics*, A. Kecskeméthy, F. Geu Flores, E. Carrera, and D. A. Elias, Eds., vol. 71. Cham, Switzerland: Springer, 2019, pp. 61–68, doi: https://doi.org/10.1007/978-3-030-90633-7
[5] R. Woodward, S. Shefelbine, R. Vaidyanathan, "Pervasive motion tracking and muscle activity monitor," in *Proc. IEEE 27th Int. Symp. Comput.-Based Med. Syst.*, 2014, pp. 421–426, doi: https://doi.org/10.1109/CBMS.2014.43
[6] F. Ennaiem et al., "Optimal design of a rehabilitation four cable-driven parallel robot for daily living activities," in *Advances in Service and Industrial Robotics*, S. Zeghloul, M. A. Laribi, and J. S. Sandoval Arevalo, Eds., vol. 84. Cham, Switzerland: Springer, 2020, pp. 3–12, doi: https://doi.org/10.1007/978-3-030-48989-2_1
[7] S. Kotov, M. Ceccarelli, M. Russo, "Design problems and requirements for assisting devices," in *New Trends in Mechanism and Machine Science*, G. Rosati, A. Gasparetto, and M. Ceccarelli, Eds., vol. 165. Cham, Switzerland: Springer, 2024, doi: https://doi.org/10.1007/978-3-031-67295-8_6
[8] M. Ceccarelli, L. Ferrara, V. Petuya, "Design of a cable-driven device for elbow rehabilitation and exercise," in *Interdisciplinary Applications of Kinematics*, A. Kecskeméthy, F. Geu Flores, E. Carrera, and D. A. Elias, Eds., vol. 71. Cham, Switzerland: Springer, 2019, pp. 61–68, doi: https://doi.org/10.1007/978-3-030-16423-2_6
[9] M. Ceccarelli, et al., "Design and experimental characterization of L-CADEL v2, an assistive device for elbow motion," *Sensors*, vol. 21, no. 15, Art. no. 5149, 2021, doi: https://doi.org/10.3390/s21155149
[10] M. Ceccarelli, S. Kotov, E. Ofonaike, M. Russo, "Test results and considerations for design improvements of L-CADEL v.3 elbow-assisting device," *Machines*, vol. 12, no. 11, Art. no. 808, 2024, doi: https://doi.org/10.3390/machines12110808
[11] S. Kotov, M. Ceccarelli, "Design and prototype of L-CADEL.v5 elbow assisting device," *Designs*, vol. 9, no. 6, Art. no. 126, 2025, doi: https://doi.org/10.3390/designs9060126
[12] D. Bizhanov, N. Zhetenbayev, A. Maksut, S. Kotov, "Elbow exoskeleton for pronation-supination motion: Modeling and prototype testing," *Bull. Civil Aviat. Acad.*, 2026, doi: https://doi.org/10.53364/24138614_2026_40_1_22
[13] H.-C. Chiu, L. Ada, "Constraint-induced movement therapy improves upper limb activity and participation in hemiplegic cerebral palsy: A systematic review," *J. Physiother.*, vol. 62, no. 3, pp. 130–137, 2016, doi: https://doi.org/10.1016/j.jphys.2016.05.013
[14] S. Dalla Gasperina, et al., "Review on patient-cooperative control strategies for upper-limb rehabilitation exoskeletons," *Front. Robot. AI*, vol. 8, art. no. 745018, 2021, doi: https://doi.org/10.3389/frobt.2021.745018
[15] D. L. Damiano, "Activity, activity, activity: Rethinking our physical therapy approach to cerebral palsy," *Phys. Ther.*, vol. 86, no. 11, pp. 1534–1540, 2006, doi: https://doi.org/10.2522/ptj.20050397
[16] M. S. Demirsoy, et al., "Development of elbow rehabilitation device with iterative learning control and internet of things," *Turkish J. Eng.*, vol. 8, no. 2, pp. 370–379, 2024, doi: https://doi.org/10.31127/tuje.1409728

Científica, vol. 30, no. 1, pp. 01-28, January-June 2026,
ISSN 2594-2921, Instituto Politécnico Nacional, MÉXICO
e300106 | DOI: 10.46842/ipn.cien.v30n1a06

[17] L. Grazi, et al., "Design and experimental evaluation of a semi-passive upper-limb exoskeleton for workers with motorized tuning of assistance," *IEEE Trans. Neural Syst. Rehabil. Eng*., vol. 28, no. 10, pp. 2276-2285, 2020, doi: https://doi.org/10.1109/TNSRE.2020.3014408
[18] S. Grosu, et al., "Driving robotic exoskeletons using cable-based transmissions: A qualitative analysis and overview," *Appl. Mech. Rev*., vol. 70, no. 6, Art. no. 060801, 2018, doi: https://doi.org/10.1115/1.4042399
[19] A. Gupta, et al., "Developments and clinical evaluations of robotic exoskeleton technology for human upper-limb rehabilitation," *Adv. Robot*., vol. 34, no. 15, pp. 1023–1040, 2020, doi: https://doi.org/10.1080/01691864.2020.1749926
[20] Z. Kadivar, C. E. Beck, R. N. Rovekamp, M. K. O'Malley, "Single limb cable driven wearable robotic device for upper extremity movement support after traumatic brain injury," *J. Rehabil. Assist. Technol. Eng*., vol. 8, 2021, doi: https://doi.org/10.1177/20556683211002448
[21] F. Molteni, G. Gasperini, G. Cannaviello, E. Guanziroli, "Exoskeleton and end-effector robots for upper and lower limbs rehabilitation: Narrative review," *PM\&R*, vol. 10, no. 9, 2018, doi: https://doi.org/10.1016/j.pmrj.2018.06.005

Científica, vol. 30, no. 1, pp. 01-28, January-June 2026,
ISSN 2594-2921, Instituto Politécnico Nacional, México
e300106 | DOI: 10.46842/ipn.cien.v30n1a06